Vulnerability of permafrost carbon to global warming. Part II: sensitivity of permafrost carbon stock to global warming

D. Khvorostyanov, Philippe Ciais, Gerhard Krinner, S. A. Zimov, C. Corradi, Georg Guggenberger

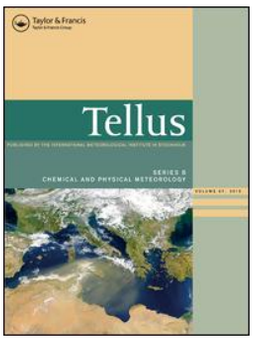

Tellus B: Chemical and Physical Meteorology

ISSN: (Print) 1600-0889 (Online) Journal homepage: https://www.tandfonline.com/loi/zelb20

Vulnerability of permafrost carbon to global warming. Part II: sensitivity of permafrost carbon stock to global warming

D. V. Khvorostyanov, P. Ciais, G. Krinner, S. A. Zimov, Ch. Corradi & G. Guggenberger

To cite this article: D. V. Khvorostyanov, P. Ciais, G. Krinner, S. A. Zimov, Ch. Corradi & G. Guggenberger (2008) Vulnerability of permafrost carbon to global warming. Part II: sensitivity of permafrost carbon stock to global warming, Tellus B: Chemical and Physical Meteorology, 60:2, 265-275, DOI: 10.1111/j.1600-0889.2007.00336.x

To link to this article: https://doi.org/10.1111/j.1600-0889.2007.00336.x

Published online: 18 Jan 2017.

Tellus (2008), 60B, 265–275
Printed in Singapore. All rights reserved

TELLUS

Vulnerability of permafrost carbon to global warming. Part II: sensitivity of permafrost carbon stock to global warming

By D. V. KHVOROSTYANOV[1,2]*, P. CIAIS[1], G. KRINNER[3], S. A. ZIMOV[4], Ch. CORRADI[5] and G. GUGGENBERGER[6], [1]*Laboratoire des Sciences du Climat et l'Environnement, Saclay, France;* [2]*A. M. Obukhov Institute of Atmospheric Physics RAS, Moscow, Russia;* [3]*Laboratoire de Glaciologie et Géophysique de l'Environnement, St Martin d'Hères, France;* [4]*Northeast Science Station, Cherskii, Russia;* [5]*UNITUS, University of Tuscia, Veterbo, Italy;* [6]*Institute of Soil Science and Plant Nutrition, Martin-Luther-Universität, Halle-Wittenberg, Germany*

(Manuscript received 22 December 2006; in final form 8 November 2007)

ABSTRACT

In the companion paper (Part I), we presented a model of permafrost carbon cycle to study the sensitivity of frozen carbon stocks to future climate warming. The mobilization of deep carbon stock of the frozen Pleistocene soil in the case of rapid stepwise increase of atmospheric temperature was considered. In this work, we adapted the model to be used also for floodplain tundra sites and to account for the processes in the soil active layer. The new processes taken into account are litter input and decomposition, plant-mediated transport of methane, and leaching of exudates from plant roots. The SRES-A2 transient climate warming scenario of the IPSL CM4 climate model is used to study the carbon fluxes from the carbon-rich Pleistocene soil with seasonal active-layer carbon cycling on top of it. For a point to the southwest from the western branch of Yedoma Ice Complex, where the climate warming is strong enough to trigger self-sustainable decomposition processes, about 256 kgC m^{-2}, or 70% of the initial soil carbon stock under present-day climate conditions, are emitted to the atmosphere in about 120 yr, including 20 kgC m^{-2} released as methane. The total average flux of CO_2 and methane emissions to the atmosphere during this time is of 2.1 kgC m^{-2} yr^{-1}. Within the Yedoma, whose most part of the territory remains relatively cold, the emissions are much smaller: 0.2 kgC m^{-2} yr^{-1} between 2050 and 2100 for Yakutsk area. In a test case with saturated upper-soil meter, when the runoff is insufficient to evacuate the meltwater, 0.05 kgCH_4 m^{-2} yr^{-1} on average are emitted as methane during 250 yr starting from 2050. The latter can translate to the upper bound of 1 GtC yr^{-1} in CO_2 equivalent from the 1 million km^2 area of the Yedoma.

1. Introduction

A large fraction of the frozen soil carbon stocks of northern latitudes are prone to disappear in a future warmer world, following permafrost thawing (e.g. Tarnocai, 1999; IPCC, 2001). Given the huge size of the frozen Arctic carbon pools, equalling roughly half that of the atmospheric carbon pool, their thawing would imply massive losses of CO_2 to the atmosphere, acting as a strong positive feedback on climate change in the next centuries. The uncertainties on the vulnerability of frozen soil carbon pools remain however very large. In particular, information is needed to estimate the rates of thawing and the threshold points above which the frozen soil carbon stores could start to decompose and to release CO_2.

There is a lack of experimental data on the decomposition rates in boreal soils, which reflect the lability of frozen soil organic matter compounds, and the extent and magnitude of frozen soil carbon stocks in Northern Siberia and North America. There are also very few modelling studies addressing the fate of frozen soil carbon in response to high-latitude global warming.

In the companion paper (Khvorostyanov et al., 2008, hereafter K08), we described a coupled soil carbon–water–energy model which deals with heat and water diffusion, CO_2 and CH_4 production in the deep soil by organic matter decomposition and methanogenesis. This model also deals with the diffusive transport of gases in the soil column, with CO_2 and CH_4 produced at depth diffusing up to the atmosphere, and atmospheric O_2 diffusing down to the depth where it is consumed by decomposition. The mobilization of frozen carbon in this model was found to

*Corresponding author.
e-mail: Dimitry.Khvorostiyanov@lsce.ipsl.fr
DOI: 10.1111/j.1600-0889.2007.00336.x

be particularly sensitive, under certain conditions, to the heat produced by soil microorganisms. Microbial heat release was shown to be a strong amplifier of atmospheric warming, capable to mobilize over 50 yr more than 20 times greater amount of carbon compared to the 'no-heating' case. Secondary effects on frozen soil carbon mobilization were caused by oxygen limitations which slow down the decomposition, and by microbial methane production which produces less heat than organic matter decomposition under oxic conditions.

The goal of this paper is to analyse the sensitivity to future atmospheric warming of the carbon stocks in the Yedoma region of North Eastern Siberia (Zimov et al., 1997; Walter et al., 2006; Zimov et al., 2006). The Yedoma Ice Complex is made of carbon-rich Pleistocene deposits, covered with more recent tundra soils. While the companion paper focused on the model theory and the role of microbial heat in the decomposition of already formed deep soil carbon stock, this manuscript considers some applications of the model, in particular to the Holocene soil and to the role of water saturation of the upper soil. This required additional model developments presented here. We added, in particular, a new module of carbon cycling in floodplain tundra ecosystems, which cap the frozen Pleistocene carbon deposits. This floodplain tundra module accounts for key methane emission processes in wetlands, which mediate the atmospheric flux of CH_4. These processes are transport by vascular plants, diffusion and ebullition. The CH_4 production under flooded conditions is calculated from litter production and plant exudation. The surface soil carbon cycling module is coupled to the deep soil model of K08 and forced by transient atmospheric warming scenarios.

In the following, we first describe the surface soil carbon module principles and new developments with respect to K08 (Section 2). We then test this model against site measurements of CH_4 fluxes at the Cherskii Northeast Science Station (Section 3), and we apply it for a point in Siberia subject to future temperature warming and precipitation changes of the SRES-A2 climate scenario of the IPSL model (Section 4). Finally, the carbon model sensitivity to its parameters is studied to determine what are the most critical factors triggering and influencing the mobilization of frozen soil carbon in the Yedoma region (Section 5). We pay attention in the discussion to the combined effects of CO_2 and CH_4 emission processes (Section 6).

2. The soil model

The 1-D model of deep frozen soil organic matter decomposition has been described in K08. The main originalities of this model are the release of heat by soil microorganisms during decomposition, and the diffusion of oxygen through the soil profile, which strongly controls decomposition. The 1-D model of soil organic matter decomposition was coupled to a permafrost model (Poutou et al., 2004). It was shown that the microbial heat release can dramatically accelerate the decomposition process. Yet, this model describing an inert stock of Pleistocene carbon-rich organic sediments exposed to warming was too idealized to be used for realistic applications, because it lacked an active ecosystem carbon cycling module in the upper part of the soil. Figure 1 shows schematically the processes described by the model.

(1) Heat conduction with account for soil moisture freezing and thawing (Poutou et al., 2004).

(2) *Soil hydrology.* The upper meter of the soil is represented by a bucket scheme. Below 1 m, the soil humidity is prescribed, using observations for Yedoma (K08).

(3) Heterotrophic respiration depending on available soil carbon, temperature and oxygen availability. Three carbon pools

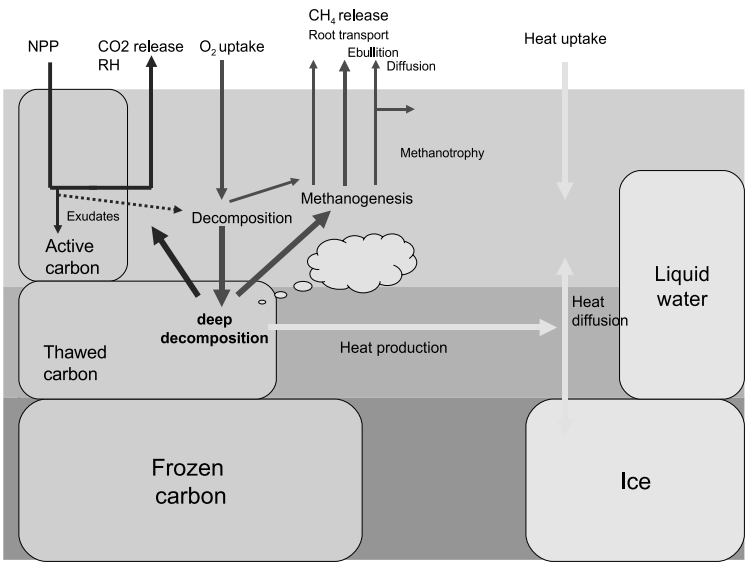

Fig. 1. Scheme of the permafrost carbon cycle model.

with different turnover times are considered. Temperature dependence is prescribed based on laboratory measurements of samples taken in Cherskii, Siberia (Chuprynin et al., 2001). Organic matter decomposition is accompanied by additional heat release into the soil (K08).

(4) Methanogenesis depending on available highly labile soil carbon as a substrate, oxygen concentration, and temperature. It is also accompanied by heat release into the soil, but the heat produced by methanogenesis is about seven times smaller than that of oxic decomposition.

(5) Methanotrophy transforming soil methane into CO_2, and producing additional heat.

(6) Vertical diffusion of oxygen and methane in the soil pores, as well as transfer of gases due to pressure differences.

(7) Methane ebullition that allows methane to avoid methanotrophy, when the gas concentration is sufficiently high.

In addition to these processes already described in K08, the current model version was improved to describe following additional key processes.

(8) *Litter decomposition.* Litter decomposition is taken from ORCHIDEE model (Krinner et al., 2005). We use here only the plant functional type of ORCHIDEE, 'C3 natural grass', which describes tundra ecosystems. We consider four litter pools: structural and metabolic, above and below ground. In order to initialize the litter pools, we take the total litter mass from an ORCHIDEE simulation under present-day climate conditions and recalculate the initial litter distribution between the pools, as well as the lignin/carbon ratio in structural litter, using the tundra root/shoot ratio for carbon allocation of 6.6 (Friedlingstein et al., 1999). After the litter content is initialized, a prescribed litter production of 75 gC m^{-2} yr^{-1}, which corresponds to tundra NPP excluding exudates (e.g. Stolbovoi and McCallum, 2002; Williams et al., 2000) is laid off every year to the soil in the end of the growing season and partitioned between litter pools according to the lignin/carbon and carbon/nitrogen ratios in leaves and roots. Part of litter is then decomposed contributing to the CO_2 flux and feeding the three soil carbon pools (see K08). The soil carbon produced by litter decomposition is distributed vertically exponentially decaying with e-folding depth z_{root}. In reality, when the soil is wet, roots can be found at maximum depths of 10–20 cm, but when the soil is dry, they can occupy the whole active layer. So the model value is $z_{\mathrm{root}} = 10$ cm for saturated soil and it increases with active layer thickness when the soil is dry. Since maximum rooting depth in tundra was found to be 50 cm (Canadell et al., 1996; Jackson et al., 1996), the e-folding depth cannot exceed 30 cm in our model.

(9) *Exudates leached from roots.* Plant roots play an important role in the supply of substrate for decomposition. According to recent studies, (e.g. Loya et al., 2002), 10–20% of tundra NPP is transformed into root exudates, which is a highly labile pool of carbon available for oxic decomposition and methanogenesis. This carbon input into the soil is generally not taken into account in NPP measurements. We assume that in addition to the estimated 75 gC m^{-2} yr^{-1} of tundra NPP, plant roots emit another 15 gC m^{-2} yr^{-1} of exudates. This easily degradable organic matter is put to the active carbon pool of the upper soil levels where roots are present.

(10) *Plant-mediated transport of methane via plant roots.* Plant-mediated transport is a mechanism that allows methane to partly avoid oxidation in soil upper levels due to its absorption by plant roots and release to the atmosphere through the plants. It is described in our model following Walter et al. (1996), Walter and Heimann (2000). In contrast to their model, we consider soil humidity that can be less then 100%. We make two additional assumptions with respect to Walter and Heimann (2000). First, we assume that the methane in air-filled pores is always in equilibrium with that dissolved in water-filled pores. Second, we assume that plant transport is proportional to soil humidity. When humidity $\theta < 1$, only a fraction θ of the soil pore volume is water-filled and can provide methane to plant roots via diffusion. The factor T_{veg} of Walter and Heimann (2000) is taken to be 10 for tundra soils, following Walter et al. (2001). Since part of methane is also oxidized near roots, plant-mediated transport decreases oxygen concentration, a prognostic variable in our model, and thus indirectly influences methanogenesis and soil organic matter decomposition.

3. Floodplain tundra soil configuration: comparison with measurements

To validate modelled CH_4 fluxes against observations, we used CH_4 flux measurements (Corradi et al., 2005) at a site located near Cherskii (161°E, 69°N). The underlying soil is a silty loam resting in the active layer or in permafrost for which we took a porosity of 0.4 corresponding to silty loam.[1] It is an alluvial material that has been deposited from the late Holocene until present. The mineral soil is covered with an organic layer of about 30–40 cm thickness, so we have chosen 36 cm as the organic layer thickness and total soil depth.

The soil was either frozen or water-saturated in summer, so that we prescribed 100% soil humidity for both thawed and frozen states. The organic layer was formed of dead leaf material, roots and rhizomes. Since carbon density and lability of this floodplain tundra soil in Cherskii area is on average the same as that of the Yedoma Pleistocene soil (unpublished data), we prescribed initial carbon density of 33 kgC m^{-3}, as well as the same proportions of active, slow, and passive soil carbon.

We could not compare the model CO_2 fluxes with observations, since the site is vegetated by sedge tussocks. The vegetation contributes strongly to the seasonal CO_2 flux due to plant respiration and photosynthesis, and these processes are not taken into account in the current version of the model. The contribution of these processes to the CO_2 flux is much larger than the

[1] http://www.sci-journal.org/index.php?template_type=report&id=11&htm=reports/vol4no2/v4n2a5.html&link=reports/home.php&c_check=1

flux caused by methanotrophy only, which occurs in our model nearly all the time since the soil is saturated.

The methane flux measurements were carried out from June 20 to September 24, 2003 using eight aluminum chambers with samplings taken once a week. The soil temperatures at 10 and 15-cm depths were measured with two sensors located in the upper part of the active layer.

Both measured and simulated 10-cm temperatures increased rapidly from about 0 °C in the beginning of June to 5 and 9 °C for measurements and the model, respectively. Measured temperature peaks in the beginning of August with 10-cm temperature reaching 12 °C and then decrease promptly in the middle of August down to about 3 °C. This August drop is less pronounced in the model with a corresponding temperature decrease from 10 to 6 °C occurring a few days later. Measured temperatures between 10 and 15 cm depth differ substantially by up to 8 °C. The simulated temperature gradient between 10 and 15-cm is considerably smaller, only about 3 °C. See Section 6 for discussion of these discrepancies.

Figure 2 shows measured and simulated methane fluxes over the period of measurements (June–September 2003). Measured fluxes show large variability between the chambers, which does not seem to be related to the effect of hummock versus hollow enclosures nor to the positioning of chambers on tussocks or between them (Corradi et al., 2005). These large variations can be related to the fact that a chamber covers a small area (0.08 m^2), so the result is affected by the large variability on spatial scales of hundred metres (corresponding to the distance at which the chambers were located). Heterogeneities in the non-decomposed underground biomass cause local differences in organic matter composition and quantity, soil and microclimate parameters such as soil porosity and temperature.

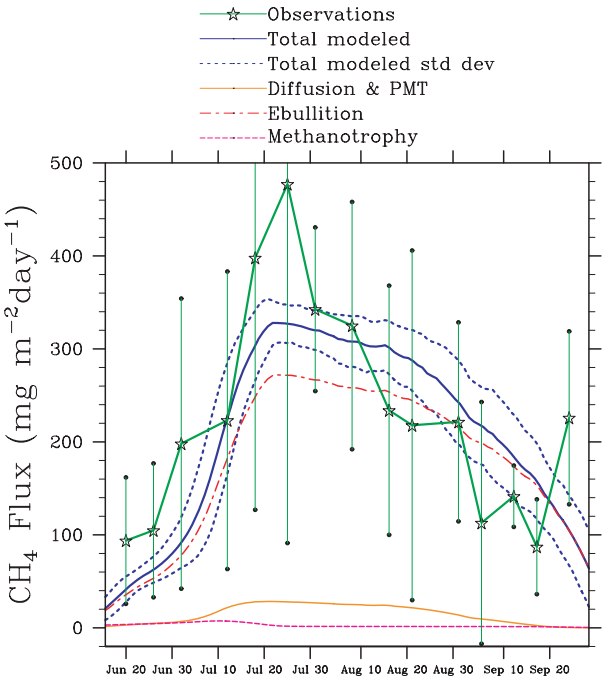

Fig. 2. Measured and simulated methane fluxes in Cherskii in summer 2003. Error bars for the measured flux present standard deviations over the eight chambers. Simulated flux is presented as the mean of 100 yr of simulation together with the standard deviations over this period. The contributions of ebullition, plant-mediated transport (the curve coincides with that for diffusion), and methanotrophy are also shown. The curve for methanogenesis contribution almost coincides with that for total CH_4 flux to the atmosphere.

The mean simulated values are in good agreement with measurements: 227 mg m^{-2} d^{-1} for the measurements and 223 mg m^{-2} d^{-1} for the model. Both fluxes show a maximum in the end of July and then diminish in the end of the season. Note that the maximum for certain individual model years can be considerably sharper than the 100-yr average flux shown in Fig. 2 and thus closer to the observed maximum (420 versus 480 mg m^{-2} d^{-1}) . In the version presented in Fig. 2 the e-folding oxygen concentration for methanogenesis O_2^* (see K08) has been changed from 2 to 3 g m^{-3} in order to better fit the seasonal maximum of the methane flux to observations. At $O_2^* = 2$ g m^{-3} the simulated maximum for individual years would lag the observed one by 10–20 d depending on a selected model year. The magnitude of the simulated peak is a little smaller than that of the measured one and would be adjustable with the methanogenesis rate parameter κ_1. In the current model version we used $\kappa_1/\kappa_2 = 9$, which is in agreement with *in situ* measurements in the eastern Siberia (see K08). Taking into account the errors in the measurements (error bars in Fig. 2), we conclude that the simulated fluxes are in a good agreement with the measured ones.

The methanogenesis curve (not shown) almost coincides with that for the total CH_4 flux in Fig. 2, since methanotrophy is almost zero, as there is no gas accumulation in the water-saturated soil. Methanogenesis is controlled by temperature and active carbon content, including exudates. As shown by Walter et al. (2006), ebullition is the primary pathway for methane to escape the soil in the Yedoma region of the eastern Siberia, in contrast to more southern sites, where the plant-mediated transport dominates (e.g. Walter and Heimann, 2000). This is reflected by the simulated fluxes shown in Fig. 2. Diffusion is mainly that through plant roots (diffusion and PMT curves in Fig. 2 coincide), since methanogenesis occurs mainly in the root layer (upper 10 cm), which is affected by plant-mediated transport.

4. Frozen Pleistocene soil carbon: response to transient warming

In K08 (Section 5) we studied the permafrost carbon cycle response to atmospheric warming in the hypothetical case of a stepwise temperature rise. The model had no active tundra carbon cycling module in the upper soil. Here we take a more realistic case of the soil response to a transient climate warming

applied for a point in Siberia (59.3°N, 101.5°E) located to the southwest from the western branch of the Yedoma Ice Complex (e.g. Sazonova et al., 2004). During the first 1000 yr, the soil model is spun up with observed climatological fields of the University of East Anglia's Climate Research Unit (CRU, http://www.cru.uea.ac.uk/, see K08). During the next 101 yr, the SRES-A2 transient climate warming scenario of the IPSL CM4 climate model (Marti et al., 2006) is applied. To reduce the influence of any bias in the climate of the IPSL CM4 model, the temperature anomalies with respect to a control unforced IPSL CM4 simulation were added to the CRU data after year 2000. We also seek to explore the long term response of permafrost carbon after 2100. To do so, we assumed climate stabilization for another 1000 yr after 2100, with climate conditions corresponding to the last year of the IPSL CM4 simulation (annual mean surface air temperature of 5 °C).

In addition to the Pleistocene soil below the active layer (about 1 m, see K08), the floodplain tundra soil carbon in the upper soil (Section 2) is also accounted for. In the course of the climate warming, the newly formed carbon in the active layer can thus contribute to further CO_2 and methane release, in addition to the deep soil carbon emissions. In contrast to the deep-soil carbon pools, however, these active layer upper carbon pools are renewable. The intensity of future CO_2 emissions from upper soil or the deep-soil carbon pools depends on mean climate conditions, as well as on the climate warming magnitude.

Figure 3 shows the profiles of the rates of gas-producing processes in the soil in summer. During normal conditions (Fig. 3a), that is, when the system has reached its equilibrium under the present-day climate, soil respiration is active only in the upper few tens of centimetres. Respiration occurs within the active layer, where soil carbon transformation to CO_2 and methane is compensated there by new carbon input from litterfall. The region of respiration activity remains confined to the surface, where there is sufficient oxygen supply. Methanotrophy also takes place near the surface at a rate few thousands times smaller than that of respiration. The mean rate of methanotrophic CO_2 production in the upper soil is of 0.08 mg m^{-3} d^{-1} (not visible in the figure). Methanotrophy occurs all the time when the temperature is positive, the atmosphere being treated as an infinite reservoir of oxygen and methane. Methane diffusing from the surface is permanently oxidized in the upper 2 m of soil.

Figure 3b shows the summer gas-producing flux profiles under a warmer climate 115 yr after the transient warming has started (year 2115). Deep soil carbon mobilization activates in response to soil warming, with methanogenesis rates climbing up to 1.25 gC m^{-3} d^{-1}, and increasing with depth below 4 m. Increased methanogenesis at depth is accompanied by increased methanotrophy in the upper soil with a peak of 1.6 gC m^{-3} d^{-1} at 2-m depth. Heterotrophic respiration reaches its maximum value of 1.8 gC m^{-3} d^{-1} at around 2.5 m depth. About 80% of the total respiration occurs below that depth, in the formerly frozen soil column (Fig. 3b).

Figure 3c and d show the corresponding profiles of oxygen and methane in the soil. The same profiles are also given for wintertime conditions. Methane concentrations are given in ppm rather

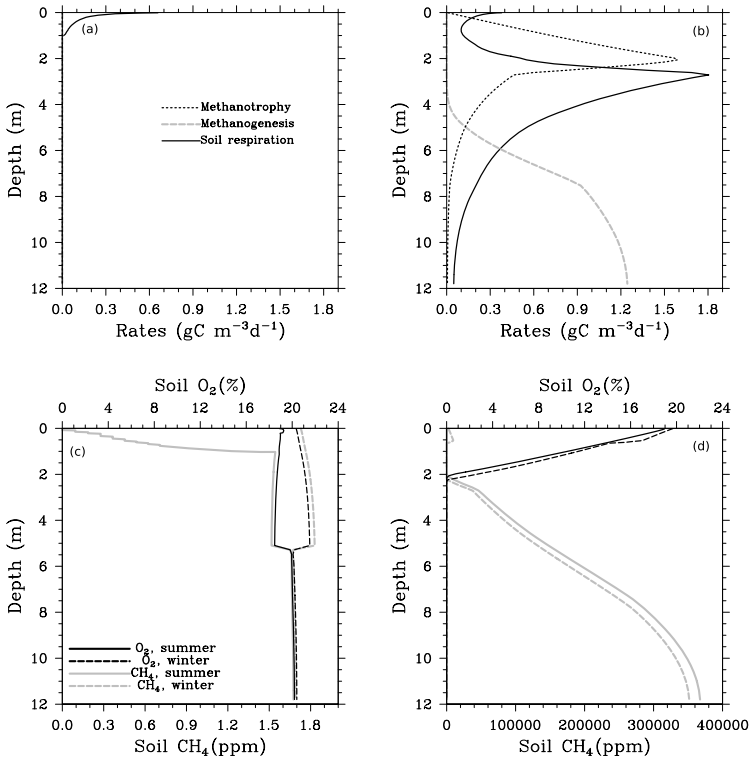

Fig. 3. Typical profiles of the rates of methanogenesis, methanotrophy, and soil respiration: (a) under present-day equilibrium conditions (year 1950); (b) in response to the external warming (year 2115). Typical profiles of oxygen and methane for winter and summer: (c) in the present-day equilibrium conditions (year 1950); (d) in response to a future transient warming (year 2115).

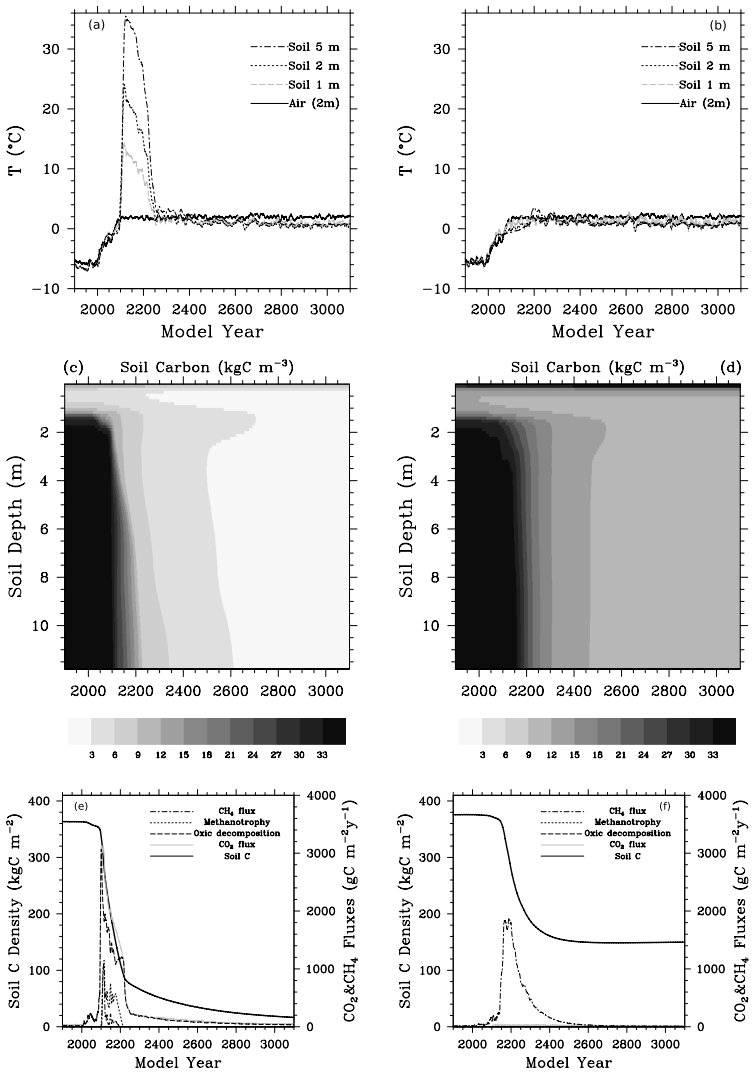

Fig. 4. (a, b): Evolution of soil temperature at various depths; (c, d): evolution of soil carbon density in kgC m^{-3} vs depth; (e, f): evolution of total soil carbon stocks (left-hand axis) and carbon fluxes (right-hand axis). The left-hand column corresponds to modelled soil humidity, as driven by rainfall changes. The right-hand column corresponds to arbitrarily prescribed 100% upper-meter humidity during the entire simulation. Air and soil temperatures are smoothed in time using running means with a window length of 10 yr. Methane and CO_2 fluxes are smoothed in time with a window length of 5 yr.

than ppb, since their values during the phase of intense methanogenesis (Fig. 3d) are extremely high. The profiles of both O_2 and CH_4 reach their minima near the surface in summer due to methanotrophy (Fig. 3c). During winter, in contrast, methanotrophy does not occur, but O_2 and CH_4 diffuse downward from the atmosphere, and their concentrations increase in the upper soil. The profiles almost merge below 5 m due to the 100% ice content of the deep soil. In the SRES-A2 warming scenario that we considered (Fig. 3d), after deep decomposition has started, soil methane increases sharply due to intense methanogenesis all year round (Fig. 4e). Methane concentration starts increasing below the depth where oxygen reaches zero (2 m). Deep CH_4 concentration during the period of most intense methanogenesis takes values of up to 370 000 ppm, which is more than 200 000 times greater than under normal, frozen, conditions! The methane concentration is so high that it can only slightly decrease during the winter, because diffusion would require several years to restore a flat soil CH_4 concentration profile.

Figure 4 shows air and soil temperatures (a, b), soil carbon (c, d), CO_2 and methane fluxes (e, f), between year 1900 and year 3100, that is, 1000 yr after temperature has stabilized by 2100. Figure 4a, c and e correspond to the reference case with soil upper meter humidity calculated by the bucket hydrology scheme. The mean value of summer-time upper-soil humidity is about 0.1. Air temperature (solid curve in Fig. 4a) rises from -5 °C before to 2 °C after 2100, and is assumed to remain stable after that date. The soil temperatures peak by year 2115, with the deepest layers being the warmest, returning to the equilibrium values (about 1 °C) during the following 100 yr. Soil temperature at 5 m depth attains 36 °C during this maximum warming phase. During this phase, most of the soil carbon is transferred into CO_2 and CH_4, with the mean carbon density integrated over the whole soil column decreasing from 33 to less than 3 kgC m^{-3} (Fig. 4c). The surface soil carbon density also diminishes from 360 to 20 kgC m^{-2} (Fig. 4e), with only 5% if the initial value remaining by year 3000. The maximum CO_2 flux attains

3200 gC m^{-2} yr^{-1} around year 2100, mainly due to 'explosive' very intense decomposition of soil organic matter (Fig. 4e). Methane emissions to the atmosphere reach up to 1200 gC m^{-2} yr^{-1}. The total amount of carbon released between 2100 and 2200 of deep-respiration phase in the form of CO_2 is about 236 kgC m^{-2} or 92%, and 20 kgC m^{-2}or 8% in the form of CH_4. The average carbon flux is 2.1 kgC $m^{-2}yr^{-1}$ during the deep respiration phase.

Figure 4b, d and f correspond to the extreme case where upper meter humidity remains prescribed to 100% reflecting the floodplain conditions of Section 3 (with additional Pleistocene carbon stock), when runoff is insufficient to evacuate all the meltwater. The range between the normal dry and the extreme saturated simulations illustrates how CO_2 and CH_4 fluxes may change under different assumptions regarding future hydrological changes in eastern Siberia. In the saturated soil simulation, the soil temperatures (Fig. 4b) do not rise to extremely high values as in Fig. 4a. Soil temperatures increase to 0 °C during the first half of transient warming, and then some additional energy is needed to thaw the permafrost. After a small peak of up to 4 °C lasting for a few decades around year 2200, the 5-m depth temperature returns gradually to its equilibrium value of 1 °C. Soil carbon decreases down to about 12 kgC m^{-3}, that is 36% of its initial value (Fig. 4d). Pleistocene carbon mobilization occurs via methanogenesis (Fig. 4f) induced by the lack of oxygen, which cannot be supplied via diffusion from the surface enough to maintain the deep respiration in flooded soils. About 40% of the deep-soil carbon stock or 142 kgC m^{-2} is transformed into CH_4 over the 100 yr of intense methanogenesis, which translates into an average flux of 1.4 or 28 kgC m^{-2} yr^{-1} in the radiative equivalent of CO_2 (see also Section 5 below). Between years 2160 and 2200, the maximum methane flux reaches 1800 gC m^{-2} yr^{-1}. These values are up to 15 times larger than the present-day fluxes measured in Cherskii (Section 3).

Thus, when runoff is not strong enough to drain efficiently meltwater in the upper-soil, the total carbon flux is about 30% less than in the reference case where soils are relatively dry in summer (with about 10% or less humidity). However all the carbon is released in the form of methane instead of CO_2, so the radiative warming effect would be an order of magnitude larger. A part of the methane released will be oxidized though in the atmosphere.

The model experiments presented above can be relevant only to marginal locations of the Yedoma, while most of its territory sustains much colder conditions. The simulations for Cherskii in the northeastern Yedoma part, with both time-varying soil humidity and saturated upper soil, do not show rapid carbon mobilization even during the A2 warming scenario. Simulations for Cherskii with saturated upper soil at present-day climate conditions yield annual methane fluxes of up to 48 gCH_4 m^{-2} yr^{-1} gradually decreasing to about 22 gCH_4 m^{-2} yr^{-1} in 500 yr. The active soil carbon density of the upper soil meter decreases at the same time from 29 to 16 kgC m^{-2} with resulting maximum methanogenesis rate decrease from 880 to 356 $mgCH_4$ m^{-3} d^{-1}. The flux values are close to those measured by Walter et al. (2006) for Yedoma thermokarst lakes (from 23 to 47 gCH_4 m^{-2} yr^{-1} for lake averages). Simulated, as well as observed, methane produced from organic sediments escapes to the atmosphere via ebullition.

5. Model sensitivity analysis

We studied the model sensitivity to its key parameters using the following experimental setup. The model was forced by present-day climate conditions in a geographical location in the central Siberia (59.3°N, 101.5°E) during 1000 yr followed by a switch to the 2 × CO_2 climate during the next 1000 yr. (The corresponding surface temperature and precipitation are shown in Fig. 5a.)

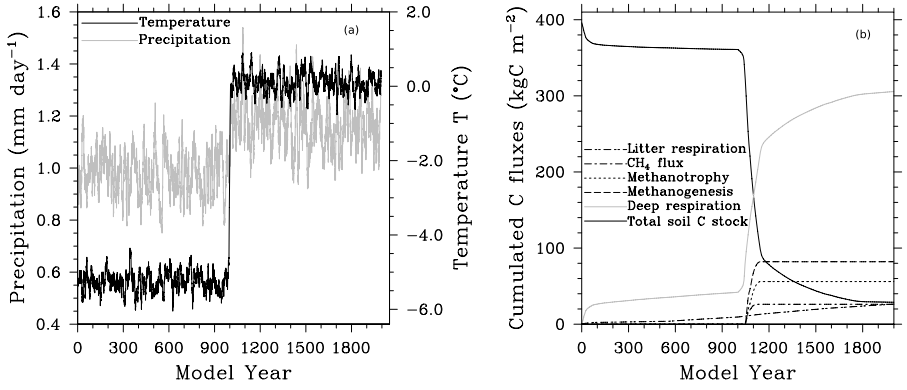

Fig. 5. Surface forcing for sensitivity analysis (a) and soil carbon balance (b). The time series in (a) have been smoothed with a window length of 10 yr. The variables in (b) are depth-integrated soil carbon (dark solid line), time-accumulated respiration (light solid), methanogenesis (long-dashed), methanotrophy (short-dashed), surface CH_4 flux (dash–dotted), and litter respiration (dash–double-dotted). The CO_2 flux (not shown) is the sum of soil respiration and methanotrophy.

The seasonal cycle (filtered out in Fig. 5a) has a quite large amplitude. The climatological mean winter (January–March) surface air temperature before the warming is −23 °C. The summer (July–September) mean temperature is 13 °C. After the warming, the winter-mean temperature becomes −16 °C, and the summer-mean temperature rises up to 16 °C. So, the winter warming is two times more pronounced than the summer one. Precipitation also increases by 19% on average in response to the warming, but its interannual variability is much higher than that of temperature.

The curves in Fig. 5b show time-accumulated fluxes of carbon transformed by methanogenesis, methanotrophy, soil respiration, and the methane flux emitted at the surface for the reference case. The figure shows how much of the soil carbon (kg m^{-2}) has been transformed by each process at a given time. The total soil carbon amount remaining before the stepwise warming is 360 kgC m^{-2}. After the 1000 yr of the 2 × CO_2 warming, only 25 kgC m^{-2} remain, i.e. $\Delta C = 335$ kgC m^{-2} has been lost by the permafrost carbon stock. About $\Delta C_{CH_4} = 27$ kgC m^{-2} have been emitted to the atmosphere as a methane flux (Fig. 5b). Fig. 5b also illustrates that cumulated oxic decomposition of soil organic matter is 320 kgC m^{-2} over the whole simulation. If one takes into account the 24 kgC m^{-2} carbon input due to litter decomposition (not shown in the figure) and initial carbon stock of 400 kgC m^{-2}, the oxic decomposition contributes 80% to the total soil carbon flux. The other sources of CO_2 are methanotrophy and litter respiration, which contribute 50 kgC m^{-2} (12%) and 30 kgC m^{-2} (8%), respectively. So the processes involving methane transformations, as well as those in the permafrost active layer, are not negligible for CO_2 fluxes.

Two of the above-mentioned quantities have been used to evaluate the model parameter sensitivity. The first one is the total cumulated CO_2 flux expressed in kmol m^{-2}. The second one is the cumulated methane flux expressed in kmol m^{-2} of CO_2 equivalent. The latter means that the methane flux has been multiplied by 20, since its radiative effect is about 20 times stronger than that of CO_2 on times scales of a century (IPCC, 2001), which is the typical time of carbon mobilization shown in Fig. 5b. Each model parameter was varied within a reasonable range of values, and the differences between the corresponding values of above-mentioned output variables were taken as sensitivity values. Table 1 lists all the parameters with respect to which the model sensitivity was explored, as well as their reference values and bounds within which they were varied. The model sensitivities with account for the radiative effect are sorted in descending order in Fig. 6. Since radiative effect of methane is much stronger than that of CO_2, the resulting model sensitivities are largely determined by the sensitivity in terms of cumulated methane flux. The order of importance of sensitive parameters is thus (Fig. 6): methane generation rate, initial carbon content, soil porosity, O_2 e-folding concentration for methanogenesis, humidity of thawed permafrost, methanotrophy time constant, etc.

Without taking into account the radiative effect, which depends on the time scale of the processes studied, the largest sensitivity of the cumulated carbon transfer is found to the initial soil carbon density C_0 (see also Fig. 7a): $\Delta C = 584$ kgC m^{-2}. Decomposition of soil organic matter (oxic and anoxic) is proportional to C_0 at a given temperature. Moreover, with more intense respiration and methanogenesis at larger C_0 values, more heat is generated, which additionally warms the soil and increases carbon mobilization. The sensitivity of carbon transfer is also high with respect to the respiration specific heat (300 kgC m^{-2}, see also Fig. 7b), soil porosity (−296 kgC m^{-2}), and soil heat conductivity changes (see Table 1).

All the 'sensitive' parameters control soil heating, freezing, and respiration and thus determine whether the carbon is mobilized due to active-layer deepening only in response to warming, or whether deep respiration and intense methanogenesis can occur and be sustained. The dependencies of carbon mobilization on these parameters are characterized by thresholds, that is, a

Table 1. Model sensitivity parameters, their reference values and variation ranges

Parameter	Reference value	Range of changes
1) Initial soil carbon density (C_0)	33.0 kgC m^{-3}	3–57
2) Specific heat of microbial oxidation to form the CO_2 (Λ_1)	40.0 MJ kgC^{-1}	10–60
3) The coefficient before the heat conductivity k[a]	1.0	0.5–2.1
4) Specific heat of methanogenesis (Λ_2)	5.5 MJ kgC^{-1}	0–20
5) Ratio of respiration rate to that of methanogenesis (κ_1/κ_2)	9	1–100
6) Methanotrophy time constant ($1/\kappa_3$)	5 d	5–100
7) Humidity of frozen deep soil (θ_i)	1.0	0.35–1.0
8) Humidity of thawed deep soil (θ_w)	0.35	0.10–0.90
9) Soil porosity (π_s)	0.5	0.2–0.9
10) Moss layer porosity (π_m)	0.92	0.70–0.99
11) O_2 e-folding concentration for methanogenesis (O_2^*)	3 g m^{-3}	0.01–10

[a]The heat conductivity has been multiplied by this factor.

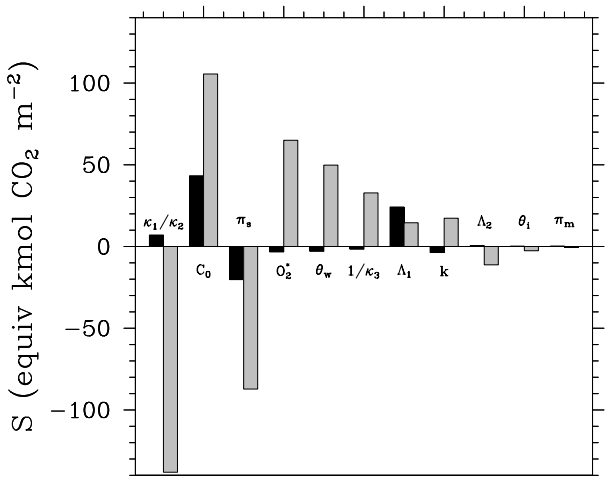

Fig. 6. Model sensitivity to variations of the following parameters was studied: initial carbon density (C_0), heat conductivity (k), respiration specific heat (Λ_1), soil porosity (π_s), moss porosity (π_m), methanogenesis rate (κ_1/κ_2), methanotrophy time constant ($1/\kappa_3$), oxygen e-folding concentration for methanogenesis (O_2^*), humidity of frozen deep soil (θ_i), humidity of thawed deep soil (θ_w), methanogenesis specific heat (Λ_2). See Table 1 and the corresponding text for explanations of the parameter meaning and values. Dark bars show the differences in the CO_2 emissions (in kmol CO_2 m^{-2}) between the two extreme parameter values. Grey bars show the same quantity but for CH_4 emissions multiplied by 20 (see comment in the text).

rapid carbon transfer increase or decrease in the vicinity of a certain parameter value. The methane flux can appear or disappear, respectively, on both sides of threshold values. An important threshold is found for the response to respiration specific heat in Fig. 7b.

Deep-soil respiration and intense methanogenesis can start only if the soil is sufficiently heated. Once started, these processes transfer much more soil carbon than the active-layer deepening only. The carbon transfer on both sides of the threshold almost completely determines the sensitivity value, that is, the difference between maximum and minimum value over the whole range of parameter values (Fig. 7b). An exception to this non-linear behaviour is the sensitivity to the initial carbon density, where the cumulated carbon transfer continues to grow substantially if C_0 is increased (Fig. 7a).

The sensitivity of the cumulated methane emissions is the highest with respect to the methanogenesis rate: $\Delta C_{CH_4} = -83$ kgC m^{-2} within the range of κ_1/κ_2 changing between 1 and 100 (see Table 1). This parameter determines the rate of methane generation in the soil and indirectly affects methanotrophy and the net methane emissions. The chosen range of parameter values is conservatively large, due to high uncertainties in methanogenesis rate. Another sensitive parameter is the initial carbon density C_0 (63 kgC m^{-2}), for the same reason as the total carbon flux. The sensitivity of the methane flux is also high with respect to the soil porosity (-52 kgC m^{-2}), which determines the amount of oxygen within the soil pores, and thus the capacity to consume it enough to maintain methanogenesis. Oxygen e-folding concentration for methanogenesis ($\Delta C_{CH_4} = 39$ kgC m^{-2}) is another sensitive parameter, since it controls at which concentration methanogenesis starts (see also Section 3). The humidity of deep-soil after thawing ($\Delta C_{CH_4} = 30$ kgC m^{-2}) also determines the space available for oxygen, while methanotrophy time constant ($\Delta C_{CH_4} = 20$ kgC m^{-2}) directly influences the rate of methane transfer into CO_2. Each of the above-mentioned parameters control either methanogenesis, or oxygen availability for it, or methanotrophy in the oxygenated upper soil and thus the surface methane flux.

6. Discussion and conclusion

A carbon cycle module describing tundra soils (seasonally dry or flooded) was added to the physical model of frozen carbon mobilization presented in K08. This allows realistic simulations of the effect of future warming on permafrost carbon at high latitudes. The new tundra soil model which accounts for methane emissions in case of flooding was run at Cherskii (Siberia) and its

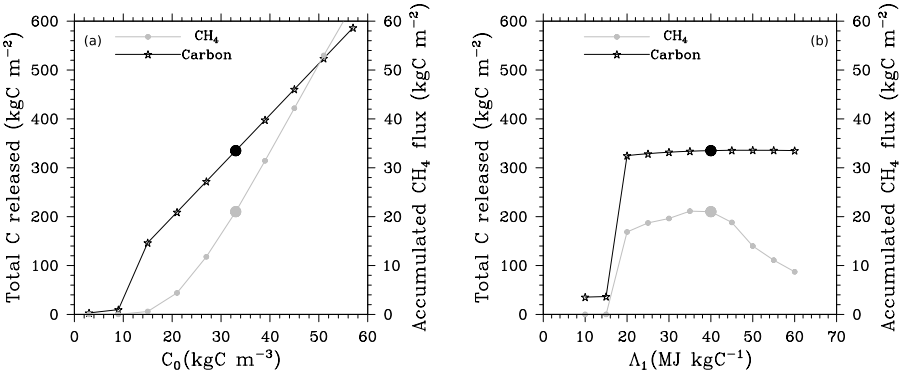

Fig. 7. Sensitivity to the initial carbon density (a) and respiration microbial heating (b). The black curve shows the sensitivity of the total carbon transformed after the warming; the grey curve shows the accumulated methane flux. Circles show the reference parameter values.

results compared favourably to in situ CH_4 flux measurements over one growing season. The vertical temperature gradient between the depths of 10 and 15 cm appears to differ from the data of temperature sensors. If the measurements of both sensors are correct, these discrepancies can imply that the model heat conductivity is overestimated. The latter would mean on the one hand that the soil is heated more rapidly and in a more homogeneous manner in summer leading to the more pronounced effect of self-sustainable deep-soil respiration (Section 4 and K08). On the other hand, increased heat conductivity leads to greater heat losses in winter, which prevents energy accumulation in the soil. At the same time, simulated methane fluxes are determined by methanogenesis in the upper 10–15 cm of soil and fairly agree with observations. So more measurements of soil vertical temperature profiles and corresponding methane fluxes, as well as similar model studies, possibly with different thermodynamic schemes are needed to clarify the issue.

We simulated surface and deep soil carbon transfer into CO_2 and methane on time scales from decades to centuries in response to climate warming, under the IPCC A2 future scenario. For a point in Siberia to the southwest from the western branch of the Yedoma, we show that about 256 kgC m^{-2}, or 70% of the initial soil carbon stock under present-day climate conditions, are mobilized in about 120 yr, including 20 kgC m^{-2} released as methane. The total average flux of CO_2 and methane emissions to the atmosphere during the most intense phase of decomposition is of 2.1 kgC m^{-2} yr^{-1}. This intense deep-soil decomposition of organic matter occurs about 70 yr after the beginning of the transient warming scenario and continues after the warming has been stabilized or even withdrawn. Once the deep-soil carbon mobilization has started, the process is irreversible because of the additional heat generated by soil microorganisms (see also K08, Section 6).

If the upper soil meter is flooded, which happens when the runoff is insufficient to withdraw the meltwater, still a half of the initial deep-soil carbon stock is transferred into CH_4 over the same period of time under the same climate conditions. This translates into 1.4 kgC m^{-2} yr^{-1} average methane flux during the 100 yr of intense methanogenesis. Taking into account the 20 times stronger radiative effect of methane, it means more than 10 times stronger warming effect with respect to the non-saturated case, or 28 kgC m^{-2} yr^{-1} in CO_2 equivalent.

Most of Yedoma territory tends to experience relatively cold conditions, too cold to trigger the self-sustaining deep-soil respiration or methanogenesis, even in the transient warming scenario studied in Section 4. This kind of simulations for Yakutsk area situated in the western part of the Yedoma would yield a maximum carbon flux of 0.2 kgC m^{-2} yr^{-1} emitted as CO_2 due to mobilization of 11 kgC m^{-2} in 50 yr with most intense soil respiration between years 2050 and 2100. When the upper soil meter is saturated, the simulation gives 0.05 $kgCH_4$ m^{-2} yr^{-1} as cumulated methane flux over 250 yr starting from 2050. Multiplied by the one-million km^2 area of Yedoma, this would translate into either 0.2 GtC yr^{-1} as CO_2 or 1 GtC yr^{-1} in CO_2 equivalent. These fluxes could provide a considerable contribution to anthropogenic greenhouse warming, which is currently about 6 GtC yr^{-1}.

Simulations for Cherskii with saturated upper soil at present-day climate conditions yield annual methane fluxes close to Walter et al. (2006). They measured strong fluxes from Yedoma thermokarst lakes of up to 130 gCH_4 m^{-2} yr^{-1} on the eroding edge, while the lake-averaged values varied between 23 and 47 gCH_4 m^{-2} yr^{-1} depending on a lake. Some aspects of this simulation setup are close to the observed conditions. The methane fluxes from thermokarst lakes are largely determined on the one hand by the quantity of newly thawed sediments and on the other hand by their lability, which decreases with time as carbon is lost to the atmosphere through ebullition. So the flux magnitude mainly results from a balance between the rate of thawed organic layer deepening under the lake and the rate of carbon loss due to methanogenesis. This balance is different for different locations in the Yedoma region, which explains large spatial variability of measured fluxes. The same balance determines the fluxes in our model. Since the main pathway for methane emissions is ebullition, methane is not oxidized on the way through the lake. The difference from the reality is that instead of a lake above the slowly thawing carbon stock we have soil active layer that freezes in winter and is exposed to high temperatures in summer. The insulating effect of moss and snow in summer and winter, respectively, decreases the seasonal cycle amplitude, but the seasonal cycle is still different from that of a thermokarst lake temperature. The two main consequences are the absence of winter methane fluxes in the model and their gradual decay while active-layer carbon stock is being mobilized. To simulate the fluxes from thermokarst lakes in a more physically founded way, one needs a lake model coupled to the soil scheme.

The amount of carbon mobilized is highly sensitive to initial carbon density, microbial respiration specific heat, soil porosity, and soil heat conductivity. Sensitivity of the accumulated CH_4 flux is high with respect to the methanogenesis rate, initial carbon density, soil porosity, oxygen e-folding concentration for methanogenesis, thawed permafrost humidity, as well as methanotrophy time constant. The dependencies of cumulated carbon fluxes on the parameters that control soil heating, freezing, and respiration are characterized by rapid increase or decrease in the vicinity of a certain threshold value. When one takes into account the 20 times stronger greenhouse effect related to methane on a century time scale, the resulting model sensitivities are largely determined by the sensitivity in terms of cumulated methane flux. The methane generation rate, initial carbon content, soil porosity, and O_2 e-folding concentration for methanogenesis are four of the most sensitive parameters in terms of equivalent CO_2 emissions. There is a need for a determination of the methane formation potential from the organic matter of the soils used as examples in this modelling effort.

Among the factors not taken into account in the current model version are changes in the ground water level, which can influence in particular methane formation and oxidation, changes in soil compaction when frozen ice thaws, as well as dependencies of soil carbon cycle parameters on availability of minerals like nitrogen and phosphorous. The latter can influence the intensity of oxic decomposition of soil organic matter.

The high sensitivity to model parameters implies that the part of the Yedoma area found in a state either on the right of thresholds similar to Fig. 7b with rapid carbon mobilization like in Fig. 4 or on the left of the thresholds with the behaviour more like Fig. 4e and f of K08, is quite sensitive to model parameters. Note that the sensitivity characteristics depend also on the choice of the ranges of parameter variations. Therefore there is a need for more measurements of permafrost carbon cycle parameters, especially the most sensitive ones. The measurements would be particularly important for the upscaling for the whole Arctic region. In situ measurements of carbon density at several metres depth, soil humidity profiles and their seasonal variations, as well as laboratory measurements of soil respiration and methanogenesis in carbon-rich permafrost regions would be utterly useful to assess the vulnerability of the Arctic frozen carbon stock.

7. Acknowledgments

The authors are grateful to Nicolas Viovy, Pierre Friedlingstein, Nathalie de Noblet, and Gilles Ramstein for useful discussions, Brigitte van Vliet-Lanoë and Almut Arneth for their expert information, Yann Meurdesoif, Julien Bruna, and Jacques Bellier for technical support, and Sébastien Denvil for help with IPSL CM4 data acquisition. D. Khvorostyanov is also grateful to Masa Kageyama and Didier Paillard for partial funding of his work (Prix Louis D. de l'Académie des Sciences 2004). The authors would like to thank as well the anonymous reviewers, whose comments have stimulated further research and new results.

References

Canadell, J., Jackson, R., Ehleringer, J., Mooney, H., Sala, O. and co-authors. 1996. Maximum rooting depth of vegetation types at the global scale. *Oecologia* **108**, 583–595.

Chuprynin, V., Zimov, S. and Molchanova, L. 2001. Modelling of thermal conditions of soils-and-grounds subject to the biological heat source. *Kriosfera Zemli* **5**(1), 80–87.

Corradi, C., Kolle, O., Walther, K., Zimov, S. A. and Schulze, E.-D. 2005. Carbon dioxide and methane exchange of a northeast Siberian tussock tundra. *Global Change Biol.* **11**(11), 1910–1925.

Friedlingstein, P., Joel, G., Field, C. B. and Fungs, I. Y. 1999. Toward an allocation scheme for global terrestrial carbon models. *Global Change Biol.* **5**, 755–770.

IPCC, 2001. *Climate Change 2001: The Scientific Basis. Contribution of Working Group I to the Third Assessment Report of the Intergovernmental Panel on Climate Change.* Cambridge University Press, Cambridge and New York.

Jackson, R., Canadell, J., Ehleringer, J., Mooney, H., Sala, O. and co-authors. 1996. A global analysis of root distributions for terrestrial biomes. *Oecologia* **108**, 389–411.

Khvorostyanov, D. V., Krinner, G., Ciais, P., Heimann, M. and Zimov, S. A. 2008. Vulnerability of permafrost carbon to global warming. Part 1. Model description and role of heat generated by organic matter decomposition. *Tellus*, **60B**, doi:11.1111/j.1600-0889.2007.00333.x.

Krinner, G., Viovy, N., de Noblet-Ducoudré, N., Ogée, J., Polcher, J. and co-authors. 2005. A dynamic global vegetation model for studies of the coupled atmosphere-biosphere system. *Global Biogeochem. Cycles* **19**, GB1015. doi:10.1029/2003GB002199.

Loya, W. M., Johnson, L. C., Kling, G. W., King, J. Y., Reeburgh, W. S. and co-authors. 2002. Pulse-labeling studies of carbon cycling in arctic tundra ecosystems: contribution of photosynthates to soil organic matter. *Global Biogeochem. Cycles* **16**(14), 1101.

Marti, O., Braconnot, P., Bellier, J., Benshila, R., Bony, S. and co-authors. 2006. The new IPSL climate system model: IPSL-CM4. Note du PÙle de Modsation 26, IPSL, F75252 Paris Cedex 5 France.

Poutou, E., Krinner, G., Genthon, C. and de Noblet-Ducoudré, N. 2004. Impact of soil freezing on future climate change. *Clim. Dyn.* **23**(6), 621–639.

Sazonova, T. S., Romanovsky, V. E., Walsh, J. E. and Sergueev, D. O. 2004. Permafrost dynamics in the 20th and 21st centuries along the East Siberian transect. *J. Geophys. Res. (Atmos.)* **109**, 1108.

Stolbovoi, V. and McCallum, I. 2002. *CD-ROM ''Land Resources of Russia"*. International Institute for Applied Systems Analysis and the Russian Academy of Science, Laxenburg, Austria.

Tarnocai, C. 1999. The effect of climate warming on the carbon balance of cryosols in Canada. *Permafrost Periglacial Process.* **10**, 251–263.

Walter, B. P., Heimann, M. and Matthews, E. 2001. Modeling modern methane emissions from natural wetlands 1. Model description and results. *J. Geophys. Res.* **106**, 34189–34206.

Walter, B. P., Heimann, M., Shannon, R. D. and White, J. R. 1996. A process-based model to derive methane emissions from natural wetlands. *Geophys. Res. Lett.* **23**, 3731–3734.

Walter, B. P., Zimov, S. A., Chanton, J. P., Verbyla, D. and Chapin, F. S. 2006. Methane bubbling from Siberian thaw lakes as a positive feedback to climate warming. *Nature* **443**, 71–75.

Walter, P. and Heimann, M. 2000. A process-based, climate-sensitive model to derive methane emissions from natural wetlands: application to five wetland sites, sensitivity to model parameters, and climate. *Global Biogeochem. Cycles* **14**(3), 745–765.

Williams, M., Eugster, W., Rastetter, E. B., Mcfadden, J. P. and Chapin, F. S. III. 2000. The controls on net ecosystem productivity along an Arctic transect: a model comparison with flux measurements. *Global Change Biol.*, **6**(s1), 116–126.

Zimov, S. A., Schuur, E. A. G. and Chapin, F. S. III. 2006. Permafrost and the Global Carbon Budget. *Science* **312**, 1612–1613.

Zimov, S. A., Voropaev, Y. V., Semiletov, I. P., Davidov, S. P., Prosiannikov, S. F. and co-authors. 1997. North Siberian lakes: a methane source fueled by Pleistocene carbon. *Science* **277**, 800–802.